

Supporting Information

On the theoretical understanding of the unexpected O₂ activation by nanoporous gold

José L. C. Fajín, M. Natália D. S. Cordeiro and José R. B. Gomes

Catalyst surfaces models and computational details

Slabs Models

A series of pure transition metal (TM=Au or Ag) surfaces [Au(111), Ag(111), Au(110), Ag(110), Ag(321) and Au(321)], doped surfaces [Au(111), Au(110) and Au(321) where some Au atoms were substituted by Ag atoms] and Ag adatoms or rows deposited on Au(111) were chosen to model at the nanoscopic level possible different microfacets of the nanoporous gold walls where O₂ dissociation was found to occur easily [1]. The pure Au(111), Ag(111), Ag(110), Au(110), Au(321) and Ag(321) surfaces were used as references for comparison of activation energies calculated on the doped surfaces and on the models considering Ag adatoms or Ag rows on Au(111). Results corresponding to the Au(321) surface were taken from Ref. [S2]. The different adsorption sites for the pure and doped TM(111) and TM(110) surfaces are as in Ref. [S3], while for the pure and doped TM(321) surfaces are as in Ref. [S2]. Results for O₂ dissociation on the pure Au(111) and Ag(111) surfaces can be found in the literature [S4] but we opted to recalculate them here for holding the computational consistency of all values that are compared in this work.

The lattice constant for bulk Au (4.1547 Å) was taken from Ref. [S2] and the lattice constant for the bulk Ag was determined through its spin-polarized-DFT energy minimization with respect to the lattice parameter using the VASP 4.6.3 computer code [S5-S6] together with the PW91 generalized gradient approach exchange correlation potential [S7], the projected augmented-wave (PAW) method [S8] as implemented in VASP [S9] to take into account the effect of core electrons in the valence electron density, a cutoff of 415 eV for the plane waves expansion and a 15×15×15 Monkhorst-Pack grid of special k-points [S10] for the numerical integration in the reciprocal space.

The lattice parameter obtained for bulk Ag using this method is 4.1547 Å. A vacuum region larger than 10 Å was introduced between repeated slabs in the z direction. The slabs correspondents to the TM(111) and TM(110) model surfaces consist of 2x2 cells with respect to the minimal unit cell while for TM(321) the 1x1 cell was used. Full relaxation was allowed for the positions of the two top metallic layers with which the oxygen species interact.

The doped surfaces were constructed by the substitution of Au atoms by Ag atoms in the pure Au surfaces and by *a posteriori* re-optimization of the atomic coordinates. The silver doped Au(111), Au(110) and Au(321) surfaces were obtained by the substitution of one, two or three Au atoms by silver atoms. In the case of the planar Au(111) surface, only a model was obtained by substitution of an Au atom in the top layer yielding the Ag@Au(111) catalyst model. In the case of the Au(110) surface, a gold atom in the outermost layer (surface combs, Fig. S1) was replaced by Ag originating the Ag@Au(110) model surface and in the case of Au(321) surface, three models were obtained: i) Ag atoms replaced Au atoms in positions 1 (see Fig. S1 for details), 2 and 5 resulting into the Ag₁@Au(321), Ag₂@Au(321) and Ag₅@Au(321) models, respectively.

Similarly, surface models were obtained where two surface gold atoms were replaced by Ag. In the case of Au(111), due to its flat nature, only atoms in the outermost layer were substituted and this procedure yielded the 2Ag@Au(111) surface). In the case of Au(110) surface, substitutions were carried out for atoms in the outermost layer (top of surface combs) yielding the 2Ag_{comb}@Au(110), for atoms in the 1st and 2nd layers, i.e., in contiguous valley and comb positions originating the 2Ag_{valley-comb}@Au(110) model, and only in the 2nd layer, i.e., in valley positions of contiguous valleys, leading to the 2Ag_{valley}@Au(110) model. Finally, for the Au(321) surface, the two Ag atoms replaced Au atoms located at the positions 1, 2 and 1, 3 and the 2Ag_{1,2}@Au(321), and 2Ag_{1,3}@Au(321) surface models, respectively, were obtained.

The models where triple atomic substitution was introduced considered only the Au(110) and Au(321) surfaces. In the former case, Ag atoms were introduced in contiguous positions, two combs and one valley, forming a triangle of silver atoms and originating the 3Ag@Au(110) model. In the latter situation, the Ag atoms substituted Au located at positions 1, 2 and 3 and the 3Ag@Au(321) surface model was obtained. In all the models described above, the two outermost metal layers were fully relaxed.

Finally, the $\text{Ag}_{\text{adatom}}@Au(111)$ and $\text{Ag}_{\text{row}}@Au(111)$ models were obtained by positioning a single Ag atom and two Ag atoms above hollow sites on the Au(111) surface, respectively. The Ag adatoms and the gold atoms into the two outermost layers were fully relaxed.

Computational details for the adsorption and transition state determinations

The interaction of O_2 (reaction initial state) and the O+O pair (reaction final state) with the models described above, modeled through the usual repeated slab approach, was studied from periodic spin polarized density functional theory (DFT) calculations. The DFT calculations for the adsorptions were carried out using the VASP code and the parameters used in the determination of the silver lattice cell constant (see above), with the exception of the Monkhorst-Pack grid of special k-points for which the energy and geometry convergences were checked for calculations on each system considered. We found that the $7 \times 7 \times 1$ Monkhorst-Pack grid of special k-points is enough to obtain a correct convergence in the energies and in the geometries. The PW91 functional was selected since after some tests in the beginning of this work showed that it yields adsorption energies and barriers similar to those computed with the PBE functional, which is in agreement with previous results calculated by us for different adsorbates and corroborated by findings in a very recent DFT-PBE study [S11].

The most stable adsorption position of the O_2 molecule in each catalytic system was considered as the initial state of the reaction and, the most stable co-adsorption position of the O+O pair as the final state of the reaction.

The transition states for the reaction of O_2 dissociation on the catalytic systems were determined using the Dimer approach [S12]. The convergence criteria were 10^{-6} eV for the total energy change and 10^{-3} eV/Å for the forces acting on the ions. We used these quite strict criteria to avoid that the algorithm converges at local minima which are numerous on the folded or stepped surface like the TM(110) and TM(321) surfaces. After the transition state localization, the computation of a single imaginary frequency for the structures obtained with the Dimer method ensures that those are true transition states. Adsorption energies, co-adsorption energies, reaction energies and energetic barriers were corrected for the *zero point vibrational energy* (ZPVE correction) using the harmonic oscillator approach.

Rate constants determination

The rate constant (k) at $T=298$ K and at $T=348$ K (temperature interval considered in the methanol oxidation on nanoporous gold [S1]) for the dissociation of O_2 on the catalytic systems mentioned above were estimated from the transition state theory [S13] as in Eq. 1

$$k = \left(\frac{k_B T}{h} \right) \left(\frac{q^\ddagger}{q} \right) e^{\frac{-E_{act}}{k_B T}} \quad (1)$$

where k_B is the Boltzmann constant, T is the absolute temperature, h is the Planck constant and E_{act} the activation energy from the ZPVE corrected calculated energy barrier. Finally, q^\ddagger and q are the partition functions for the TS and initial state, respectively, which have been approximated from the harmonic vibrational frequencies.

Table S1. DFT calculated parameters for O₂ dissociation on the catalytic systems proposed.

Surface	$E_{\text{ads}}^{\text{e}}(\text{O}_2)$ ^[a]	$E_{\text{ads}}^{\text{o}}(\text{O}_2)$ ^[b]	$E_{\text{ads}}^{\text{c}}(\text{O} + \text{O})$ ^[c]	$E_{\text{ads}}^{\text{o}}(\text{O} + \text{O})$ ^[d]	$E_{\text{react}}^{\text{e}}$ ^[e]	$E_{\text{react}}^{\text{o}}$ ^[f]	$E_{\text{act}}^{\text{e}}$ ^[g]	$E_{\text{act}}^{\text{o}}$ ^[h]	ν_i ^[i]	$\text{O}\cdots\text{O}$ _[j]	k (298 K) ^[k]	k (348 K) ^[l]
Au(111)	-0.01	0.00	0.71	0.74	0.71	0.74	1.93	1.90	376	1.97	1.37×10 ⁻²¹	5.81×10 ⁻¹⁷
Ag(111)	-0.14	-0.14	0.02	0.05	0.16	0.19	1.06	1.04	425	1.92	4.12×10 ⁻⁰⁷	1.34×10 ⁻⁰⁴
Ag@Au(111)	-0.03	-0.04	0.56	0.59	0.59	0.63	1.70	1.69	379	2.01	2.03×10 ⁻¹⁶	3.99×10 ⁻¹²
2Ag@Au(111)	-0.04	-0.04	0.37	0.40	0.41	0.44	1.27	1.25	438	1.91	1.45×10 ⁻¹⁰	1.64×10 ⁻⁰⁷
Au(110)	-0.19	-0.18	0.41	0.41	0.60	0.59	0.85	0.83	403	1.80	2.08×10 ⁻⁰³	2.06×10 ⁻⁰¹
Ag(110)	-0.63	-0.63	-1.30	-1.29	-0.67	-0.66	0.52	0.51	364	1.98	3.88×10 ⁺⁰³	6.88×10 ⁺⁰⁴
Ag@Au(110)	-0.30	-0.29	0.17	0.19	0.47	0.47	0.86	0.83	362	1.87	1.48×10 ⁻⁰³	1.49×10 ⁻⁰¹
2Ag _{comb} @Au(110)	-0.39	-0.38	-0.16	-0.15	0.22	0.23	0.95	0.93	301	1.96	1.26×10 ⁻⁰⁴	2.49×10 ⁻⁰²
2Ag _{valley} @Au(110)	-0.23	-0.22	0.07	0.08	0.30	0.30	0.59	0.56	422	1.75	3.90×10 ⁺⁰²	1.03×10 ⁺⁰⁴
Charged ^[m]	(-0.37)	(-0.36)	(0.04)	(0.02)	(0.42)	(0.38)	(0.58)	(0.57)	(497)	1.81	(5.09×10 ⁺⁰²)	(1.44×10 ⁺⁰⁴)
2Ag _{valley-comb} @Au(110)	-0.33	-0.31	0.08	0.08	0.40	0.40	0.60	0.57	365	1.85	5.33×10 ⁺⁰¹	1.25×10 ⁺⁰⁴
Charged ^[m]	(-0.55)	(-0.53)	(-0.28)	(-0.27)	(0.26)	(0.26)	(0.64)	(0.60)	(395)	1.81	(7.53×10 ⁺⁰¹)	(2.55×10 ⁺⁰⁴)
3Ag@Au(110)	-0.41	-0.40	-0.59	-0.57	-0.18	-0.17	0.66	0.64	316	1.96	1.11×10 ⁺⁰¹	4.39×10 ⁺⁰²
Au(321) ^[n]	-0.17	-0.16	-0.35	-0.31	0.05	0.08	1.00	0.96	620	1.91	5.46×10 ⁻⁰⁵	1.21×10 ⁻⁰²
Ag(321)	-0.49	-0.48	-1.09	-1.07	-0.61	-0.60	0.53	0.52	339	1.98	7.59×10 ⁺⁰²	1.31×10 ⁺⁰⁴
Ag ₁ @Au(321)	-0.28	-0.27	0.07	0.09	0.35	0.36	1.09	1.07	217	2.12	1.99×10 ⁻⁰⁷	7.54×10 ⁻⁰⁵
Ag ₂ @Au(321)	-0.30	-0.28	-0.46	-0.42	-0.16	-0.14	1.26	1.22	253	2.00	6.53×10 ⁻¹⁰	6.12×10 ⁻⁰⁷
Ag ₃ @Au(321)	-0.22	-0.20	-0.31	-0.27	-0.10	-0.07	1.16	1.13	337	1.91	3.88×10 ⁻⁰⁸	2.07×10 ⁻⁰⁵
2Ag _{1,2} @Au(321)	-0.39	-0.38	-0.27	-0.25	0.12	0.13	1.16	1.14	200	2.08	5.13×10 ⁻⁰⁸	3.38×10 ⁻⁰⁵
2Ag _{1,3} @Au(321)	-0.37	-0.36	-0.50	-0.46	-0.12	-0.10	0.95	0.93	339	1.97	1.94×10 ⁻⁰⁵	3.44×10 ⁻⁰³
3Ag@Au(321)	-0.49	-0.48	-0.62	-0.60	-0.13	-0.12	0.89	0.87	283	2.07	3.16×10 ⁻⁰³	4.50×10 ⁻⁰¹
Ag _{adatom} @Au(111)	-0.31	-0.31	0.49	0.49	0.81	0.80	1.05	1.03	393	2.08	2.67×10 ⁻⁰⁶	9.97×10 ⁻⁰⁴
Ag _{row} @Au(111)	-0.72	-0.71	-0.53	-0.49	0.19	0.22	0.86	0.82	428	1.90	3.63×10 ⁻⁰³	4.05×10 ⁻⁰¹
Charged ^[m]	(-0.97)	(-0.95)	(-0.95)	(-0.92)	(0.02)	(0.03)	(0.91)	(0.86)	(438)	1.88	(3.77×10 ⁻⁰³)	(5.34×10 ⁻⁰¹)

[a] O₂ adsorption energy in eV; [b] ZPVE corrected O₂ adsorption energy in eV; [c] O+O adsorption energy in eV; [d] ZPVE corrected O+O adsorption energy in eV; [e] reaction energy in eV; [f] ZPVE corrected reaction energy in eV; [g] activation energy barrier in eV; [h] ZPVE corrected activation energy barrier in eV; [i] imaginary frequency; [j] O₂ breaking bond in Å; [k] reaction rate constant (s⁻¹) at 298 K; [l] reaction rate constant (s⁻¹) at 348 K; [m] results for the charged surfaces; [n] the data corresponding to this surface were calculated from the geometries of Ref. (S2).

Table S2. Adsorption energies (E_{ads} , eV) and structural parameters (d , Å) for the adsorption of the O₂ on pure and derived TM(111) surfaces.^a

O ₂ adsorption					
Surface	Position ^b	E_{ads}^e	$d_{O_a-surf}^c$	$d_{O_b-surf}^c$	O ₂ bond length ^d
Au(111)	top	not stable			
	bridge	not stable			
	hole hcp – hole fcc	not stable			
	physisorbed ^e	-0.01	3.59	3.16	1.24
Ag(111)	top	not stable			
	bridge	-0.14	2.39	2.39	1.30
	hole hcp – hole fcc	not stable			
Ag@Au(111)	top Ag	not stable			
	bridge Ag-Au	not stable			
	bridge Au-Au	not stable			
	physisorbed ^e	-0.03	4.19	3.56	1.24
2Ag@Au(111)	top Ag	not stable			
	top Au	not stable			
	bridge Ag-Au	not stable			
	bridge Au-Au	not stable			
	bridge Ag-Ag	-0.04	2.54	2.54	1.27
	physisorbed ^e	-0.02	3.28	3.72	1.24
Ag_{adatom}@Au(111)	top Ag (2 Ag-O bonds)	-0.27	2.41	2.41	1.29
	bridge Ag-Au	it moves to top Ag			
	Top Ag (1 Ag-O bond)	-0.31	2.16	3.02	1.28
	bridge Au-Au	it moves to “top Ag – top Ag”			
	top Ag – top Ag	-0.06	2.50	2.51	1.34
Ag_{row}@Au(111)	bridge Ag-Ag	-0.72	2.23	2.23	1.32
	bridge Au-Au	it moves to bridge Ag-Ag			

^aThe adsorption energies correspond to electronic adsorption energies.

^bSee nomenclature in Fig. S3.

^cDistance from oxygen atoms to the nearest surface atom.

^dLength of the internal O₂ bond.

^eA physisorbed state is considered for adsorbate to surface distances larger than 3 Å.

Table S3. Adsorption energies (E_{ads} , eV) and structural parameters (d , Å) for the adsorption of the O+O pair on pure and derived TM(111) surfaces.^a

O+O adsorption				
Surface	Position ^b	E_{ads}^e	$d_{O_a-surf}^c$	$d_{O_b-surf}^c$
Au(111)	bridge – bridge		adsorbates move to hole fcc – hole fcc	
	bridge – hole hcp		adsorbates move to hole hcp – hole hcp	
	bridge – hole fcc		adsorbates move to hole fcc – hole fcc	
	hole fcc – hole fcc	0.71	2.05, 2.05, 2.24	2.05, 2.05, 2.24
	hole fcc – hole hcp	1.47	2.15, 2.15, 2.14	2.19, 2.19, 2.21
	hole hcp – hole hcp	0.87	2.14, 2.13, 2.13	2.13, 2.13, 2.13
Ag(111)	bridge – bridge		adsorbates move to hole fcc – hole hcp	
	bridge – hole hcp		adsorbates move to hole fcc – hole hcp	
	bridge – hole fcc		adsorbates move to hole fcc – hole fcc	
	hole fcc – hole fcc	0.08	2.12, 2.12, 2.13	2.12, 2.12, 2.12
	hole fcc – hole hcp	0.02	2.00, 2.16, 2.16	2.15, 2.00, 2.15
	hole hcp – hole hcp	0.49	2.19, 2.19, 2.06	2.18, 2.06, 2.19
Ag@Au(111)	hole fcc – hole fcc*	0.64	2.08, 2.20, 2.08	2.13, 2.13, 2.10
	hole fcc* – hole fcc*	0.56	2.10, 2.09, 2.18	2.18, 2.10, 2.09
	hole fcc* – hole hcp*	0.69	2.16, 2.16, 2.04	2.15, 2.03, 2.15
	hole fcc – hole hcp	1.22	2.20, 2.22, 2.20	2.14, 2.14, 2.15
	hole hcp – hole hcp*	0.87	2.12, 2.12, 2.16	2.14, 2.11, 2.14
	hole hcp* – hole hcp*	0.83	2.10, 2.19, 2.06	2.09, 2.09, 2.19
2Ag@Au(111)	hole fcc* – hole hcp*	0.62	2.19, 2.19, 2.04	2.06, 2.21, 2.20
	hole fcc* – hole fcc	0.42	2.16, 2.06, 2.15	2.17, 2.10, 2.8
	hole fcc – hole hcp	0.37	2.03, 2.14, 2.14	2.03, 2.20, 2.20
	hole fcc – hole fcc	0.49	2.12, 2.12, 2.18	2.14, 2.13, 2.17
Ag_{adatom}@Au(111)	hole adatom - hole fcc		adsorbates move to hole adatom – hole adatom	
	hole adatom – hole hcp		adsorbates move to hole adatom – hole adatom	
	hole adatom – hole adatom	0.49	2.17, 2.21, 2.15	2.18, 2.27, 2.28
Ag_{row}@Au(111)	hollow(4) – hollow(3)		adsorbates move to hollow(4) – bridge	
	hollow(4) – bridge Ag-Ag	-0.36	2.40, 2.09, 2.40, 2.09	2.00, 2.00
	bridge Ag-Ag – hollow(3)	-0.63	1.98, 1.98	2.04, 2.14, 2.04

^aThe adsorption energies correspond to electronic adsorption energies.

^bSee nomenclature in Fig. S3.

^cDistance from the oxygen to the nearest surface atoms.

Table S4. Adsorption energies (E_{ads} , eV) and structural parameters (d, Å) for the adsorption of the O₂ on pure and derived TM(110) surfaces.^a

O ₂ adsorption					
Surface	Position ^b	E_{ads}^c	$d_{O_a-surf}^c$	$d_{O_b-surf}^c$	O ₂ bond length ^d
Au(110)	top	not stable			
	long-bridge	-0.07	2.21	2.21	1.33
	hollow(4)	not stable			
	short-bridge	-0.18	2.30	2.30	1.30
Ag(110)	top	not stable			
	long-bridge				
	hollow(4)	-0.63	2.36, 2.37	2.36, 2.37	1.46
	short-bridge	-0.53	2.28	2.31	1.32
Ag@Au(110)	top Ag	not stable			
	hollow(4)	not stable			
	bridge Ag-Au	-0.30	2.34	2.25	1.31
2Ag_{comb}@Au(110)	top Ag	-0.05	2.64	2.62	1.27
	hollow(4)	-0.05	2.46, 2.46	2.44, 2.48	1.39
	bridge Ag-Ag	-0.39	2.31	2.31	1.31
2Ag_{valley}@Au(110)	top Ag	not stable			
	hollow(4)	not stable			
	bridge Au-Au	-0.23	2.28	2.28	1.31
2Ag_{valley-comb}@Au(110)	top Ag	not stable			
	hollow(4)	-0.12	2.44, 2.42	2.41, 2.48	1.30
	bridge Ag-Au	-0.33	2.32	2.23	1.31
3Ag@Au(110)	top Ag	-0.05	2.63	2.62	1.27
	hollow(4)	adsorbates move to bridge Ag-Ag			
	bridge Ag-Ag	-0.41	2.29	2.30	1.27

^aThe adsorption energies correspond to electronic adsorption energies.

^bSee nomenclature in Fig. S4.

^cDistance from oxygen atoms to the nearest surface atoms.

^dLength of the internal O₂ bond.

Table S5. Adsorption energies (E_{ads} , eV) and structural parameters (d , Å) for the adsorption of the O+O pair on pure and derived TM(110) surfaces.^a

O+O adsorption				
Surface	Position ^b	E_{ads}^e	$d_{O_a-surf}^c$	$d_{O_b-surf}^c$
Au(110)	hollow(3-up) – hollow(3-up)	0.67	2.18, 2.17, 2.21	2.18, 2.17, 2.21
	hollow(3-down) – long-bridge	0.41	2.24, 2.25, 2.25	2.04, 2.04
	hollow(3-down) – hollow(3-down)	adsorbates move to hollow(3-down) – long-bridge		
Ag(110)	hollow(3-up) – hollow(3-up)	-1.30	2.13, 2.13, 2.21	2.13, 2.13, 2.21
	hollow(3-down) – hollow(3-down)	-1.26	2.32; 2.33, 2.08	2.08, 2.32, 2.33
Ag@Au(110)	hollow(3-up) – hollow(3-up)	0.58	2.16, 2.17, 2.26	2.17, 2.16, 2.26
	hollow(3-down) – hollow(3-down)	adsorbates move to hollow(3-down) – long-bridge		
	hollow(3-down) – long-bridge	0.16	2.04, 2.22, 2.22	2.12, 1.96
2Ag_{comb}@Au(110)	hollow(3-up) – hollow(3-up)	0.44	2.28, 2.26, 2.13	2.25, 2.26, 2.13
	hollow(3-down) – hollow(3-down)	adsorbates move to hollow(3-down) – long-bridge		
	hollow(3-down) – long-bridge	-0.16	2.06, 2.34, 2.21	2.18, 2.04
2Ag_{valley}@Au(110)	hollow(3-up) – hollow(3-up)	0.07	2.16, 2.16, 2.25	2.17, 2.16, 2.25
	hollow(3-down) – hollow(3-down)	0.33	2.39, 2.09, 2.42	2.08, 2.43, 2.39
2Ag_{valley-comb}@Au(110)	hollow(3-down) – hollow(3-down)	adsorbates move to hollow(3-down) – long-bridge		
	hollow(3-up) – hollow(3-up)	0.25	2.19, 2.18, 2.12	2.46, 2.25, 2.22
	hollow(3-down) – long-bridge	0.08	2.27, 2.26, 2.30	2.01, 2.16
3Ag@Au(110)	hollow(3-down) – hollow(3-down)	-0.05	2.39, 2.34, 2.12	2.39, 2.48, 2.12
	hollow(3-up) – hollow(3-up)	-0.59	2.08, 2.08, 2.37	2.12, 2.12, 2.21

^aThe adsorption energies correspond to electronic adsorption energies.

^bSee nomenclature in Fig. S4.

^cDistance from the oxygen to the nearest surface atoms.

Table S6. Adsorption energies (E_{ads} , eV) and structural parameters (d , Å) for the adsorption of the O₂ on pure and derived TM(321) surfaces.^a

O ₂ adsorption					
Surface	Position ^b	E_{ads}^e	$d_{O_a-surf}^c$	$d_{O_b-surf}^c$	O ₂ bond length ^d
Au(321)^e	top 1 – b ₁₋₃	-0.10	2.41	4.03	1.26
	top 1	-0.14	2.41	3.22	1.26
	top 1 – b ₁₋₄	-0.12	2.26	3.96	1.27
	b ₁₋₂	-0.17	2.23	2.38	1.31
	b ₂₋₁	-0.14	2.33	2.29	1.31
Ag(321)	b ₁₋₂	-0.41	2.29	2.36	1.31
	b ₂₋₁	-0.49	2.28	2.31	1.32
	b ₃₋₄	-0.27	2.38	2.44	1.36
Ag₁@Au(321)	b ₁₋₂	-0.28	2.30	2.30	1.31
	b ₂₋₁	-0.26	2.29	2.28	1.31
	physisorbed ^f	-0.09	3.72	3.44	1.25
	b ₃₋₄	not stable			
Ag₂@Au(321)	b ₁₋₂	-0.30	2.22	2.38	1.31
	b ₂₋₁	-0.26	2.31	2.23	1.31
	b ₃₋₄	not stable			
Ag₃@Au(321)	b ₁₋₂	-0.22	2.23	2.34	1.31
	b ₂₋₁	-0.12	2.33	2.29	1.30
	physisorbed ^f	-0.01	2.95	3.32	1.26
	b ₃₋₄	not stable			
2Ag_{1,2}@Au(321)	b ₃₋₄	not stable			
	b ₂₋₁	-0.37	2.30	2.27	1.31
	b ₁₋₂	-0.39	2.27	2.31	1.31
2Ag_{1,3}@Au(321)	physisorbed ^f	-0.09	3.83	3.29	1.27
	b ₃₋₄	not stable			
	b ₂₋₁	-0.37	2.25	2.26	1.32
	b ₁₋₂	-0.34	2.27	2.31	1.32
3Ag@Au(321)	b ₁₋₂	-0.46	2.24	2.33	1.31
	b ₂₋₁	-0.49	2.28	2.25	1.32
	b ₃₋₄	-0.01	2.38	2.48	1.34

^aThe adsorption energies correspond to electronic adsorption energies.

^bSee nomenclature in Ref S2.

^cDistance from oxygen atoms to the nearest surface atoms.

^dLength of the internal O₂ bond.

^eThese data were taken from Ref. S2.

^fA physisorbed state is considered for adsorbate to surface distances larger than 3 Å.

Table S7. Adsorption energies (E_{ads} , eV) and structural parameters (d , Å) for the adsorption of the O+O pair on pure and derived TM(321) surfaces.^a

O+O adsorption				
Surface	Position ^b	E_{ads}^e	$d_{O_a-surf}^c$	$d_{O_b-surf}^c$
Au(321)^d	hole "a" – b ₁₋₄	-0.23	2.01	1.96
	hole "d" – hole "h"	-0.35	2.01	2.02
Ag(321)	hole "a" – hole "d"	-0.93	2.01, 2.16, 2.08	2.14, 2.28, 2.62
	hole "a" – hole "g"	-1.08	2.04, 2.19, 2.13	2.28, 2.17, 2.11, 2.77
	hole "a" – hole "e"	-1.09	2.04, 2.14, 2.20	2.27, 2.18, 2.23
	hole "b" – hole "c"	-0.79	2.09, 2.33, 2.34	2.27, 2.49, 2.46
	hole "b" – hole "e"	-0.94	2.14, 2.16, 2.04	2.09, 2.26, 2.24
	hole "b" – hole "h"	-0.90	2.12, 2.04, 2.23	2.27, 2.18, 2.06
Ag₁@Au(321)	hole "a" – b ₄₋₁	0.07	2.07, 2.12, 2.18	2.13, 2.06,
	hole "a" – hole "g"	adsorbates move to hole "a" – b ₄₋₁		
	hole "a" – hole "h"	0.34	2.28, 2.13, 2.08	2.36, 2.21, 2.18
	hole "b" – hole "c"	0.53	2.17, 2.13, 2.13	2.06, 2.43, 2.14
	hole "b" – hole "g"	0.59	2.13, 2.14, 2.25	2.15, 2.28, 2.56, 2.47
	hole "b" – hole "h"	0.42	2.10, 2.24, 2.08	2.34, 2.13, 2.15
Ag₂@Au(321)	hole "a" – hole "g"	adsorbates move to hole "a" – b ₄₋₁		
	hole "a" – b ₄₋₁	-0.45	2.01, 2.19, 2.13	2.08, 1.97
	hole "a" – hole "h"	0.47	2.16, 2.28, 2.09	2.16, 2.27, 2.22
	hole "b" – hole "c"	0.28	2.06, 2.25, 2.16	2.34, 2.13, 2.06
	hole "b" – hole "g"	0.66	2.13, 2.12, 2.25	2.47, 2.14, 2.21, 2.73
	hole "b" – hole "h"	-0.05	2.00, 2.23, 2.18	2.00, 2.35, 2.26
Ag₃@Au(321)	hole "a" – hole "g"	adsorbates move to hole "a" – b ₄₋₁		
	hole "a" – b ₄₋₁	-0.29	2.02, 2.20, 2.11	2.07, 1.96
	hole "a" – hole "h"	0.42	2.10, 2.17, 2.24	2.09, 2.17, 2.41
	hole "b" – hole "c"	0.63	2.09, 2.16, 2.17	2.07, 2.16, 2.47
	hole "b" – b ₂₋₁	0.66	2.09, 2.32, 2.19	2.10, 2.07
	hole "b" – hole "h"	-0.08	1.98, 2.10, 2.57	2.01, 2.42, 2.20
2Ag_{1,2}@Au(321)	hole "a" – hole "h"	adsorbates move to hole "a" – hole "g"		
	hole "a" – b ₄₋₁	-0.27	2.04, 2.20, 2.15	2.15, 2.07
	hole "a" – hole "g"	-0.18	2.12, 2.15, 2.08	2.12, 2.15, 2.44
	hole "b" – hole "c"	0.19	2.13, 2.23, 2.10	2.05, 2.35, 2.13
	hole "b" – hole "g"	0.20	2.09, 2.20, 2.24	2.51, 2.25, 2.43, 2.21
	hole "b" – hole "h"	0.08	2.08, 2.16, 2.16	2.09, 2.45, 2.15
2Ag_{1,3}@Au(321)	hole "a" – hole "d"	-0.50	2.07, 2.13, 2.05	2.05, 2.11, 2.12
	hole "a" – hole "g"	adsorbates move to hole "a" – hole "e"		
	hole "a" – hole "e"	-0.23	2.09, 2.08, 2.23	2.38, 2.17, 2.39
	hole "b" – hole "c"	adsorbates move to hole "b" – hole "g"		
	hole "b" – hole "e"	-0.23	2.18, 2.09, 2.08	2.17, 2.07, 2.25
	hole "b" – hole "h"	-0.08	2.06, 2.28, 2.06	2.07, 2.18, 2.25
3Ag@Au(321)	hole "a" – hole "d"	-0.62	2.02, 2.17, 2.18	2.11, 2.33, 2.07
	hole "a" – hole "g"	adsorbates move to hole "a" – hole "e"		
	hole "a" – hole "e"	-0.52	2.04, 2.19, 2.14	2.35, 2.46, 2.16
	hole "b" – hole "c"	-0.15	2.01, 2.36, 2.15	2.46, 2.40, 2.15
	hole "b" – hole "e"	-0.51	2.16, 2.05, 2.13	2.08, 2.23, 2.18

^aThe adsorption energies correspond to electronic adsorption energies.

^bSee nomenclature in Ref S2.

^cDistance from oxygen atoms to the nearest surface atoms.

^dThese data were taken from Ref. S2.

Table S8. Computed Bader charges (a.u.) for the oxygen atoms in the initial (IS), transition (TS) and final (FS) states on the Au(111) and Agrow@Au(111) model catalysts.

Catalyst model	IS	TS	FS
Au(111)	-0.259 / -0.257	-0.524 / -0.545	-0.745 / -0.743
Agrow@Au(111)	-0.270 / -0.313	-0.590 / -0.624	-0.734 / -0.871

Fig. S1. Representation of the substitution sites on the Au(111), Au(110) and Au(321) surfaces for the elaboration of the doped surfaces.

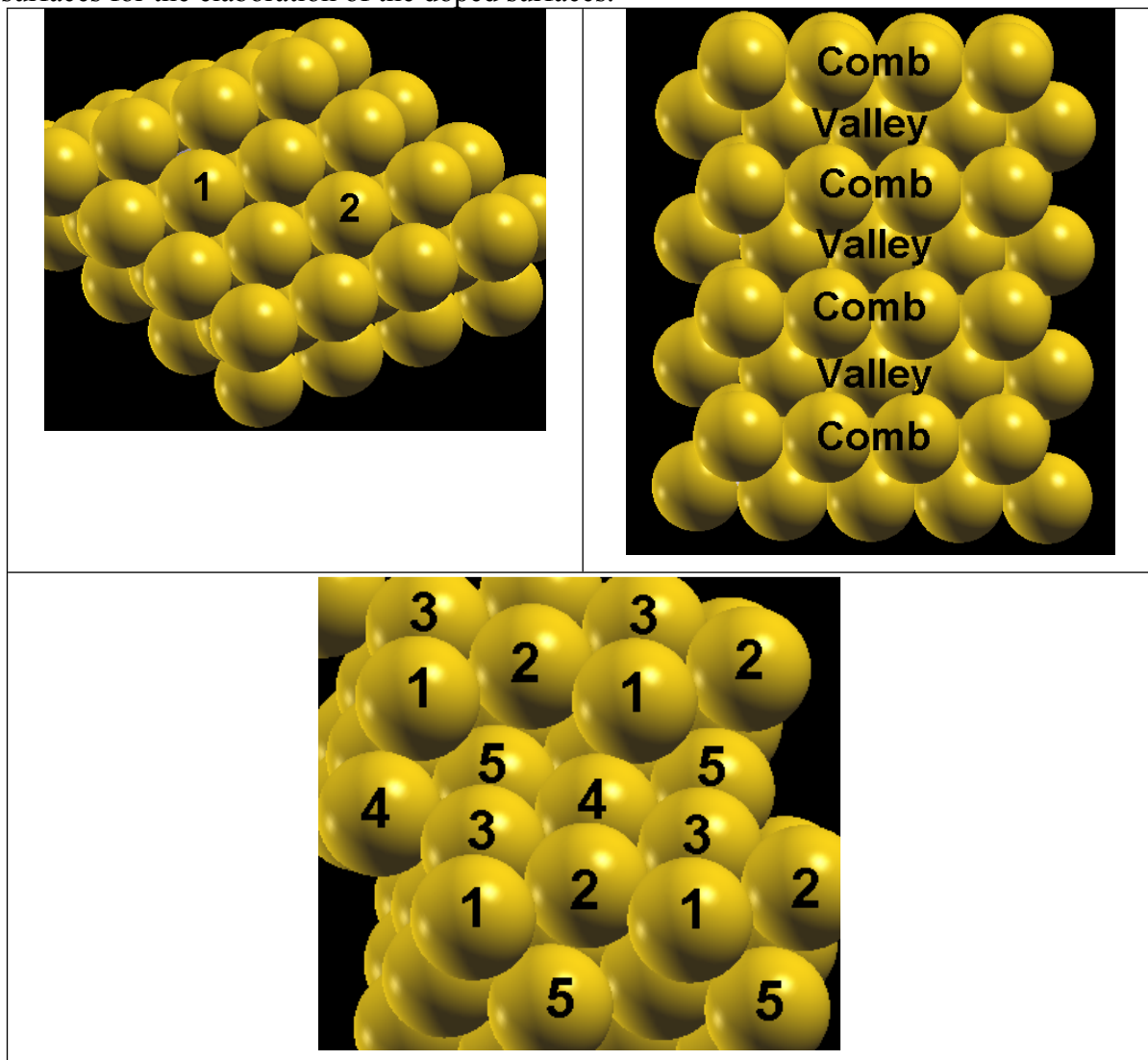


Fig. S2. Representation of the most favorable reaction paths for the O₂ dissociation on the different catalyst models considered in this work.

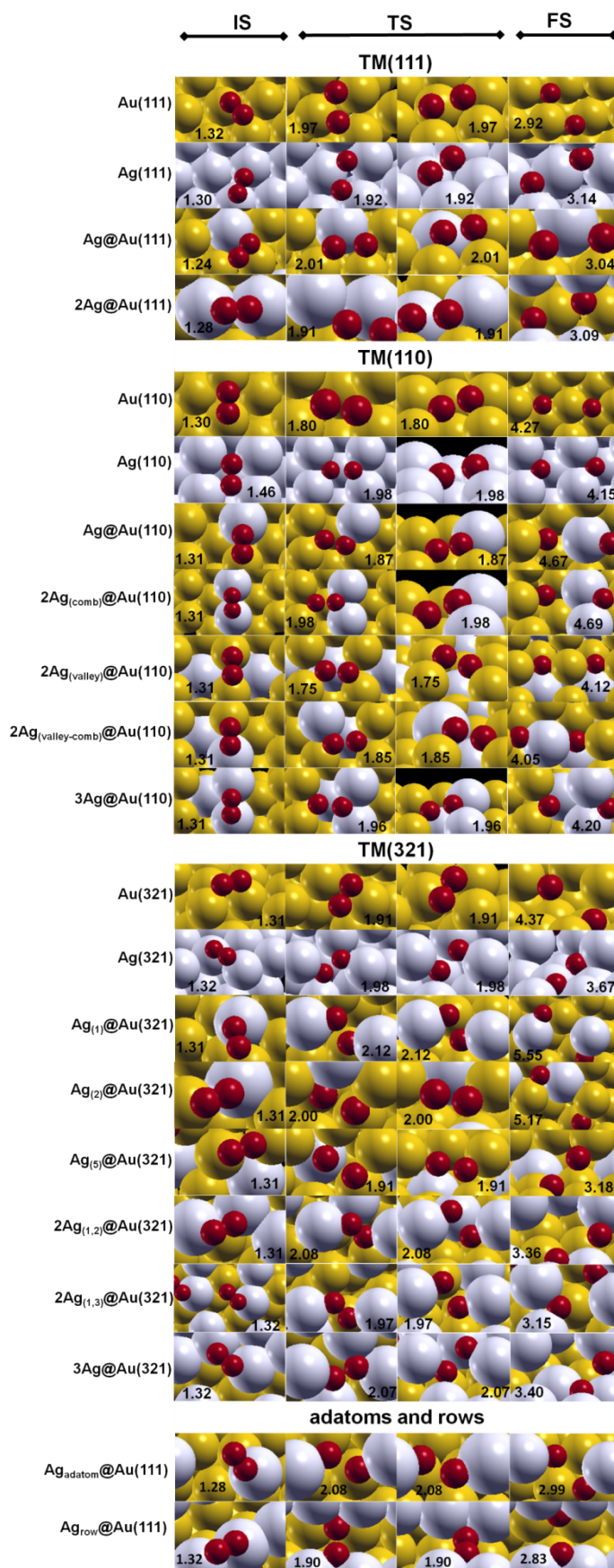


Fig. S3. Nomenclature used for the pure and derived TM(111) surfaces.

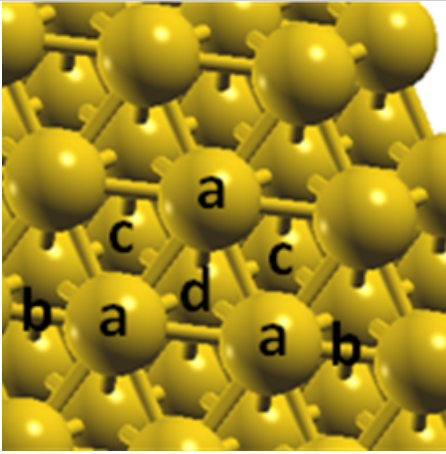
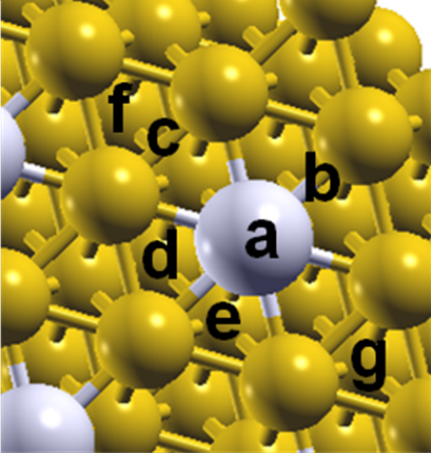
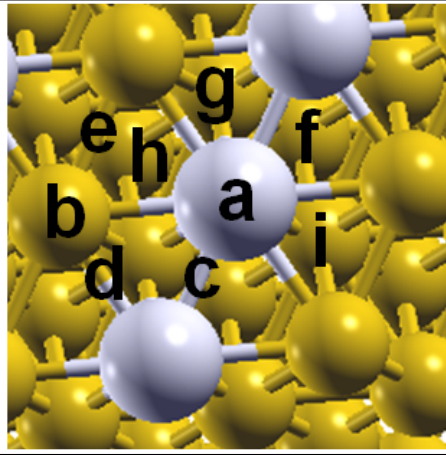
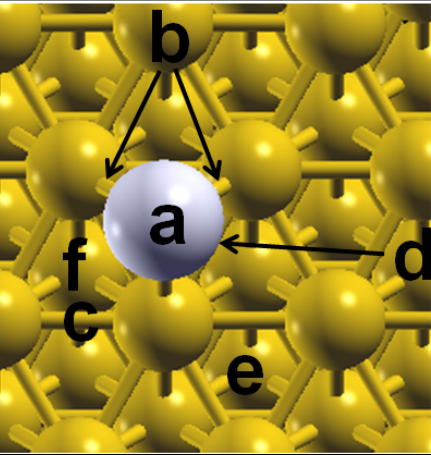
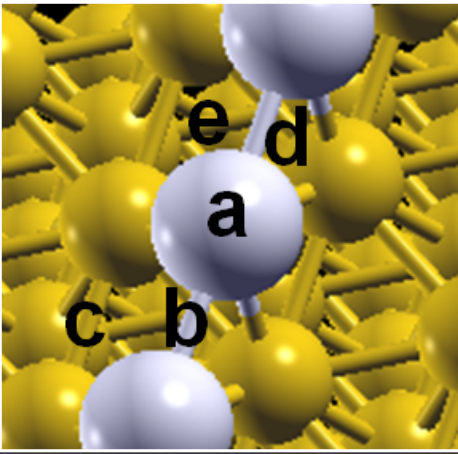
	
<p>Pure TM(111) surfaces: a) top; b) bridge; c) hole fcc; and d) hole hcp.</p>	<p>Ag@Au(111) surface: a) top Ag; b) bridge Ag-Au; c) bridge Au-Au; d) hole fcc*; e) hole hcp*; f) hole fcc; and g) hole hcp.</p>
	
<p>2Ag@Au(111) surface: a) top Ag; b) top Au; c) bridge Ag-Ag; d) bridge Ag-Au; e) bridge Au-Au; f) hole fcc*; g) hole hcp*; h) hole fcc; and i) hole hcp.</p>	<p>Ag_{adatom}@Au(111) surface: a) top Ag; b) bridge Ag-Au; c) bridge Au-Au; d) hole adatom; e) hole fcc; and f) hole hcp.</p>
	
<p>Ag_{row}@Au(111) surface: a) top Ag; b) bridge Ag-Ag; c) bridge Au-Au; d) hollow(3); and e) hollow(4).</p>	

Fig. S4. Nomenclature used for the pure and derived TM(110) surfaces.

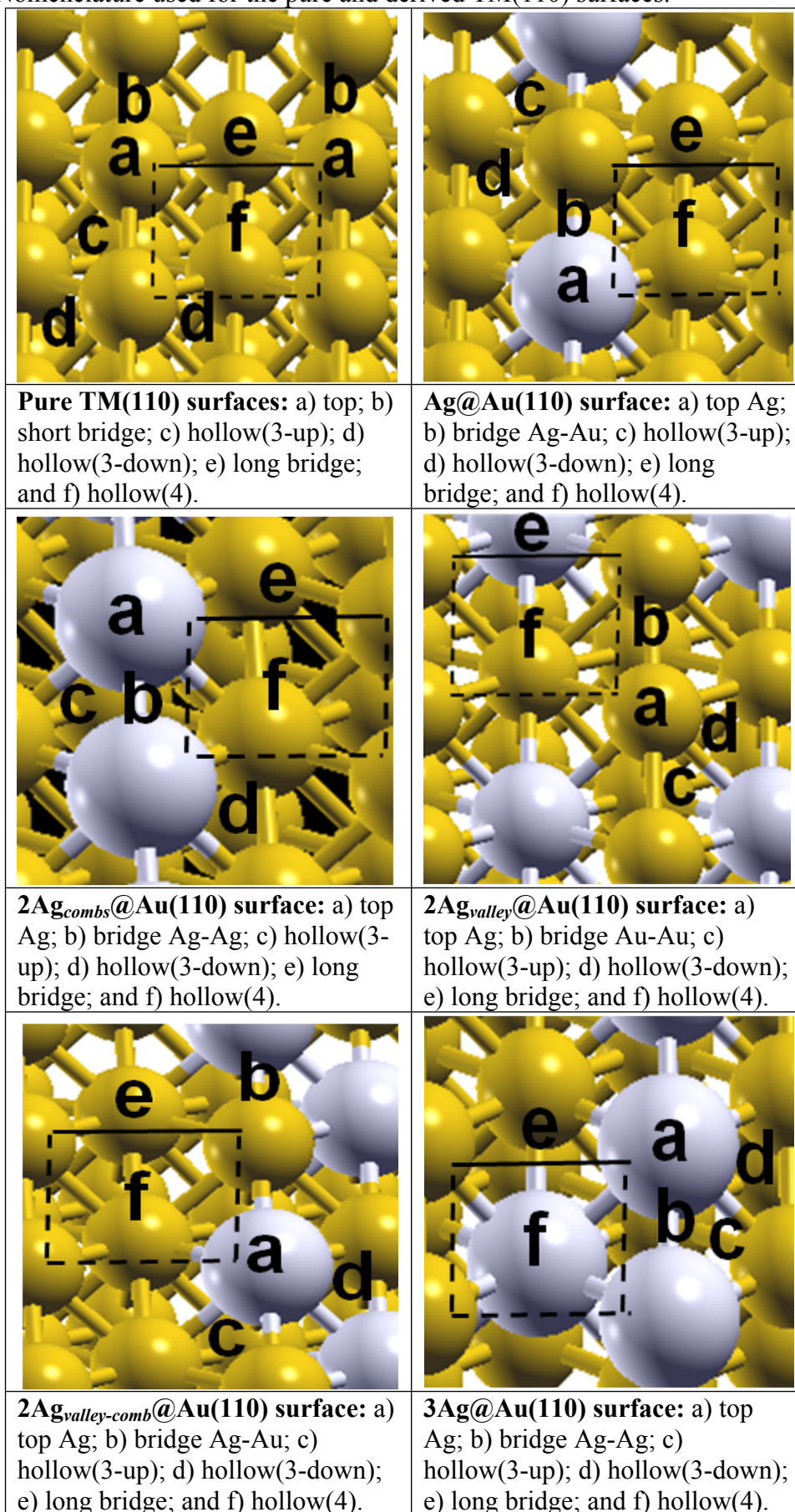
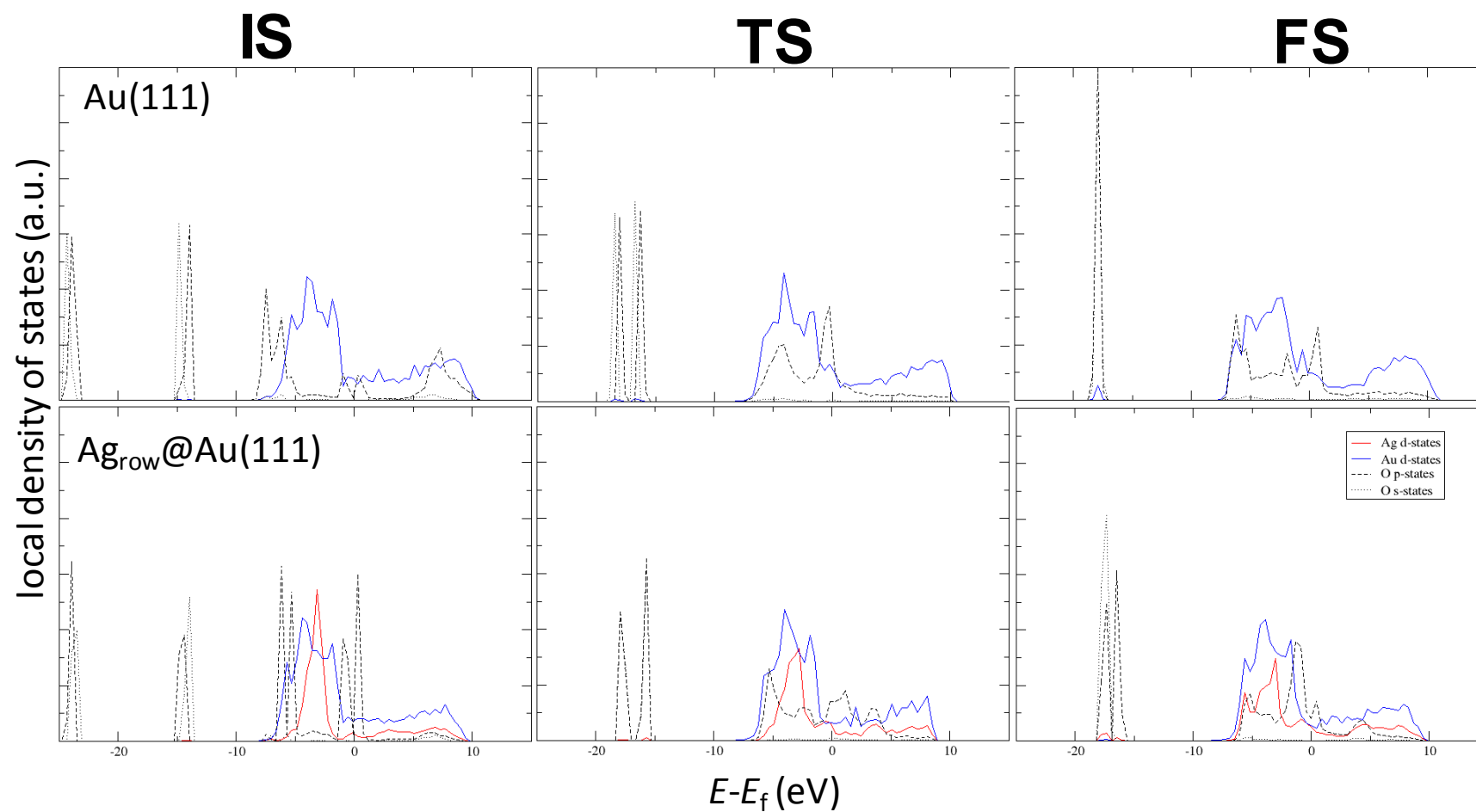


Fig. S5. Local density of states for the initial (IS), transition (TS) and final (FS) states on the Au(111) and Ag_{row}@Au(111) model catalysts.



Acknowledgements: We thank Fundação para a Ciência e a Tecnologia, FCT, FEDER and Fundo Social Europeu for financial support. We thank FCT for grant SFRH/BPD/64566/2009 given to JLCF and for Programa Ciência 2007.

REFERENCES

- (S1) A. A. Wittstock, V. Zielasek, J. Biener, C. M. Friend and M. Bäumer, *Science*, 2010, **327**, 319.
- (S2) J. L. C. Fajín, M. N. D. S. Cordeiro, J. R. B. Gomes, *J. Phys. Chem. C*, 2007, **111**, 17311.
- (S3) A. M. Pessoa, J. L. C. Fajín, J. R. B. Gomes, M. N. D. S. Cordeiro, *J. Mol. Struct. Theochem*, 2010, **946**, 43.
- (S4) W. -L. Yim, T. Klüner, *J. Catal.*, 2008, **254**, 349.
- (S5) G. Kresse, J. Hafner, *Phys. Rev. B*, 1993, **47**, 558.
- (S6) G. Kresse, J. Furthmüller, *Phys. Rev. B*, 1996, **54**, 11169.
- (S7) J. P. Perdew, J. A. Chevary, S. H. Vosko, K. A. Jackson, M. R. Pederson, D. J. Singh, C. Fiolhais, *Phys. Rev. B*, 1992, **46**, 6671.
- (S8) P. E. Blöchl, *Phys. Rev. B* 1994, **50**, 17953.
- (S9) G. Kresse, D. Joubert, *Phys. Rev. B* 1999, **59**, 1758.
- (S10) H. J. Monkhorst, J. D. Pack, *Phys. Rev. B* 1976, **13**, 5188.
- (S11) L. V. Moskaleva, S. Röhe, A. Wittstock, V. Zielasek, T. Klüner, K. M. Neyman and M. Bäumer, *Phys. Chem. Chem. Phys.*, 2011, **13**, 4529.
- (S12) G. Henkelman, H. Jónsson, *J. Chem. Phys.*, 1999, **111**, 7010.
- (S13) K. J. Laidler, in *Chemical Kinetics* third ed., Harper Collins, New York, 1987. p 193.